



CHALMERS
UNIVERSITY OF TECHNOLOGY

Gradual emergence of superconductivity in underdoped La_{2-x} Sr_x CuO₄















Downloaded from: <https://research.chalmers.se>, 2024-11-05 13:07 UTC

Citation for the original published paper (version of record):

Țuțueanu, A., Kamminga, M., Tejsner, T. et al (2023). Gradual emergence of superconductivity in underdoped La_{2-x} Sr_x CuO₄. Physical Review B, 107(17).
<http://dx.doi.org/10.1103/PhysRevB.107.174514>

N.B. When citing this work, cite the original published paper.

Gradual emergence of superconductivity in underdoped $\text{La}_{2-x}\text{Sr}_x\text{CuO}_4$

Ana-Elena Țuțueanu ^{1,2}, Machteld E. Kamminga ^{1,*}, Tim B. Tejsner ^{1,2}, Henrik Jacobsen ^{1,3}, Henriette W. Hansen,¹
 Monica-Elisabeta Lăcătușu,^{1,3} Jacob Baas ⁴, Kira L. Eliassen ^{1,5}, Jean-Claude Grivel ⁶, Yasmine Sassa ⁷,
 Niels Bech Christensen ⁸, Paul Steffens ², Martin Boehm ², Andrea Piovano ², Kim Lefmann ¹
 and Astrid T. Rømer ^{1,9,†}

¹Nanoscience Center, Niels Bohr Institute, University of Copenhagen, 2100 Copenhagen, Denmark

²Institut Laue-Langevin, 38042 Grenoble, France

³Paul Scherrer Institute, Laboratory for Neutron Scattering and Imaging, 5232 Villigen, Switzerland

⁴Zernike Institute for Advanced Materials, University of Groningen, 9747 AG Groningen, The Netherlands

⁵Glass and Time, IMFUFA, Department of Science and Environment, Roskilde University, 4000 Roskilde, Denmark

⁶Department of Energy Conversion and Storage, Technical University of Denmark, 2800 Kgs. Lyngby, Denmark

⁷Department of Physics, Chalmers University of Technology, 412 96 Göteborg, Sweden

⁸Department of Physics, Technical University of Denmark, 2800 Kgs. Lyngby, Denmark

⁹Danish Fundamental Metrology, Kogle Allé 5, 2970 Hørsholm, Denmark



(Received 3 November 2022; revised 7 February 2023; accepted 30 March 2023; published 15 May 2023)

We present triple-axis neutron scattering studies of low-energy magnetic fluctuations in strongly underdoped $\text{La}_{2-x}\text{Sr}_x\text{CuO}_4$ with $x = 0.05, 0.06$ and 0.07 , providing quantitative evidence for a direct competition between these fluctuations and superconductivity. At dopings $x = 0.06$ and $x = 0.07$, three-dimensional superconductivity is found, while only a very weak signature of two-dimensional superconductivity residing in the CuO_2 planes is detectable for $x = 0.05$. We find a surprising suppression of the low-energy fluctuations by an external magnetic field at all three dopings. This implies that the response of two-dimensional superconductivity to a magnetic field is similar to that of a bulk superconductor. Our results provide direct evidence of a very gradual onset of superconductivity in cuprates.

DOI: [10.1103/PhysRevB.107.174514](https://doi.org/10.1103/PhysRevB.107.174514)

I. INTRODUCTION

The emergence of unconventional superconductivity is closely connected to other electronic ordering phenomena, such as spin- and charge-density modulations [1]. In the simplest family of cuprate superconductors, antiferromagnetic order of the insulating parent compound La_2CuO_4 is suppressed by doping, and superconductivity emerges upon further doping [2,3]. In the low-doping regime, spin- and charge-stripe order coexist with superconductivity and here, superconducting critical temperatures remain modest with $T_c \leq 20$ K. In general, low-energy magnetic fluctuations appear to be antagonists to superconductivity [4] and the opening of a gap in the magnetic energy spectrum is observed in cuprate superconductors only when these become doped to optimal critical temperature. For $\text{La}_{2-x}\text{Sr}_x\text{CuO}_4$ (LSCO), this happens at a doping of $x \gtrsim 0.14$ [5,6].

An external magnetic field applied to optimally doped LSCO generates in-gap states [7] and eventually completely

closes the superconducting gap [5]. In contrast, moderately underdoped LSCO ($x \sim 0.10$) shows no spin gap and no field effect on the low-temperature, low-energy excitations [8]. While there is consensus that optimally doped cuprates exhibit homogeneous d -wave superconductivity [9], the nature of superconductivity within the stripe-ordered phase on the underdoped side of the phase diagram is still being debated; is superconductivity phase separated from stripe-ordered regions or do these coexist? Coexistence of stripes and superconducting order, in which the latter is spatially modulated to accommodate the spin stripes, is found in $\text{La}_{2-x}\text{Ba}_x\text{CuO}_4$ (LBCO) [2,10–12]. This phase, called the pair-density-wave (PDW) phase, was also proposed on theoretical grounds in order to describe multiple intertwined orders in the low-doping regime of the cuprates [13–15]. Phase-sensitive signatures of the PDW phase in LBCO was recently presented in Ref. [11]. In this material, the onset of diamagnetism occurs at temperatures above the bulk T_c for magnetic fields applied perpendicular to the CuO_2 planes [10]. For magnetic fields parallel to the planes, no diamagnetism is observed which is interpreted as an interplanar frustration of the Josephson coupling preventing three-dimensional d -wave superconductivity from developing. Besides the growing evidence of a PDW phase in LBCO, scanning tunneling microscopy on the related material, $\text{Bi}_2\text{Sr}_2\text{CaCu}_2\text{O}_{8+x}$, found direct evidence of a modulated superconducting order parameter [18].

It is tempting to ask if spatially modulated superconductivity is a universal player encountered on the route to superconductivity in the cuprate family. To approach this

*Currently at: Condensed Matter and Interfaces, Debye Institute for Nanomaterials Science, Utrecht University, 3508 TA Utrecht, The Netherlands.

†asr@dfm.dk

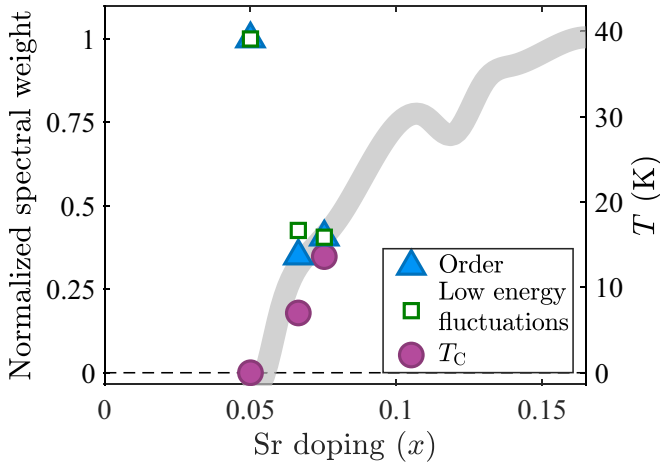


FIG. 1. The evolution of magnetic order, low-energy fluctuations and superconducting T_c as a function of doping. T_c of our crystals (determined from SQUID measurements) is shown in magenta and the change in magnetic order and low-energy fluctuations ($\hbar\omega = 0.8$ meV), quantified by the neutron scattering spectral weight, is shown by blue triangles and green squares, respectively. The gray line displays the evolution of T_c as determined in Refs. [7,8,16,17].

question, we focus on LSCO in the underdoped region near the onset of superconductivity ($x_c = 0.055$) [19].

We first show that, for $x < x_c$, this material displays weak two-dimensional superconducting correlations, a precursor to bulk superconductivity occurring at doping values above x_c . Next, we study the low-energy magnetic fluctuations and magnetic order using neutron scattering. Figure 1 shows one of our main findings: The elastic and low-energy inelastic (0.8 meV) spin correlation functions as a function of doping, together with the superconducting transition temperatures. It is clear that both the elastic and inelastic neutron signals drastically decrease at the onset of superconductivity. This is direct evidence of competition between superconductivity and low-energy fluctuations.

Finally, we show that the response to an external magnetic field does not depend on whether bulk superconductivity is established in the material or not. Our results provide evidence of a very gradual emergence—rather than an abrupt onset—of superconductivity in LSCO.

II. EXPERIMENTAL METHOD

We investigated three LSCO crystals with nominal dopings of $x = 0.05$ (LSCO5), 0.06 (LSCO6), and 0.07 (LSCO7). The crystals were grown by the traveling-solvent floating-zone method [20], and the precise doping was inferred from the transition temperature between the high-temperature tetragonal and the low-temperature orthorhombic phases [21], yielding $x = 0.050(2)$, $0.0664(6)$, and $0.0753(3)$, for LSCO5, LSCO6, and LSCO7, respectively. In the crystal with the lowest doping, LSCO5, susceptibility measurements in a magnetic field applied perpendicular to the CuO_2 planes find a weak but clear diamagnetic response (blue data points in Fig. 2). We interpret this as the formation of screening currents within the CuO_2 planes in small parts of the sample at temperatures below 4.2 ± 0.3 K, consistent with previous reports

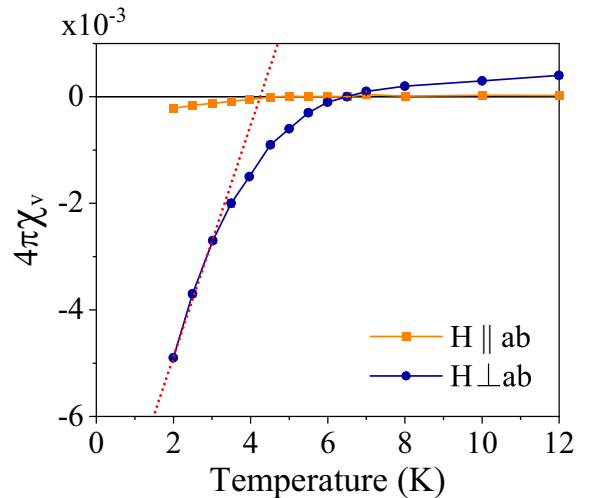


FIG. 2. Magnetic volume susceptibility measured in LSCO5 with a small magnetic field ($H = 2$ mT) applied parallel and perpendicular to the (a, b) plane. These measurements were performed while heating, preceded by zero field cooling (ZFC). A weak diamagnetic response sets in at the characteristic temperature of 4.2 ± 0.3 K displayed by the dotted red line.

on the presence of superconducting fluctuations in underdoped cuprates [22,23]. On the other hand, superconducting correlations between the planes are strongly suppressed and only an extremely weak response is found for fields applied parallel to the CuO_2 planes (orange data points in Fig. 2). This response is most likely caused by a minor misalignment, resulting in a small field component perpendicular to the planes. More details are given in the Supplemental Material (SM) [24]. The superconducting transition temperatures of LSCO6 ($T_c = 7.0 \pm 0.4$ K) and LSCO7 ($T_c = 13.6 \pm 0.2$ K) are determined from susceptibility measurements on small, crushed pieces of the corresponding large single crystals used for the neutron studies presented throughout this paper, see the SM for more details [24]. For both samples, we find that the diamagnetic response is far from that of a perfect diamagnet at $T = 2$ K, indicating that a sizable fraction of the samples remains nonsuperconducting at this temperature. The increase of T_c upon doping is shown by the magenta points and the gray curve in Fig. 1. Critical temperatures at higher doping values are inferred from the literature [7,8,16,17]. We note that the width of the line is a reflection of the spread in the reported T_c values. To study the incommensurate magnetic order and fluctuations, we performed several experiments on the cold neutron triple-axis spectrometer ThALES [25] at Institut Laue-Langevin (ILL) [26–29]. We used the standard setting of the instrument, employing a velocity selector before the doubly focusing monochromator to suppress second-order contamination and a Beryllium-filter before the horizontally focusing analyzer to reduce background. No collimation was used. In addition, we performed one experiment on the thermal triple-axis spectrometer IN8 at ILL [30], using a Si(111) monochromator, see the SM [24] for details.

The samples were placed in 10 T (LSCO5 and LSCO7) and 15 T (LSCO6) vertical field cryomagnets and slowly cooled with a 1 K/min rate down to 100 K and fast cooled afterwards.

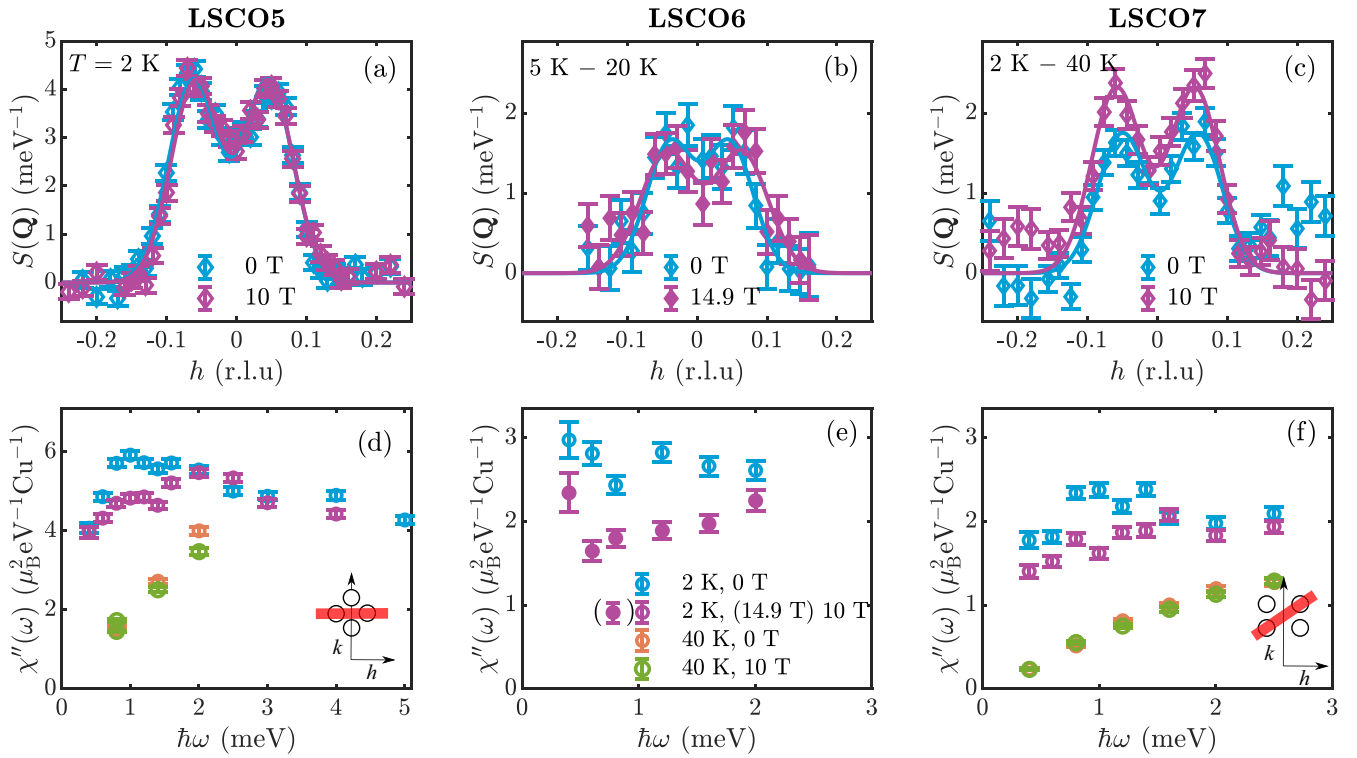


FIG. 3. (a)–(c) Spin correlation $S(\mathbf{Q})$ of background subtracted elastic signals with (purple) and without (blue) applied magnetic field of the samples LSCO5, LSCO6, and LSCO7, respectively. The solid lines are Gaussian fits as explained in the text. (d)–(f) Brillouin Zone averaged dynamic susceptibility $\chi''(\omega)$ measured at 2 K at zero field (blue circles) with an applied magnetic field of 10 T (purple circles), and at 40 K at zero field (orange circles) and with an applied magnetic field of 10 T (green circles). For the LSCO6 sample, the magnetic field was 14.9 T (represented by the filled purple circles). The inset in (d) illustrates the scan direction used for the LSCO5 sample, while the inset in (f) shows the scan direction for the LSCO6 and LSCO7 samples.

The outgoing wave vector, $k_f = 1.55 \text{ \AA}^{-1}$, was kept constant across the different experiments, since this value was found to be free of unwanted double scattering events [31]. During data acquisition on ThALES, the energy resolution was $\Delta E \sim 0.15 \text{ meV}$ (FWHM) in the elastic condition and increased up to $\sim 0.3 \text{ meV}$ for the inelastic scans, depending on the energy transfer. In the standard focusing condition applied in these experiments, the momentum resolution in the horizontal scattering plane was $\Delta Q \sim 0.02 \text{ \AA}^{-1}$.

With the c axis vertical, scattering wave vectors $\mathbf{Q} = (h, k, 0)$ were accessible in the horizontal scattering plane. Wave vectors are expressed in units of $(2\pi/a, 2\pi/b, 2\pi/c)$ with the measured low-temperature lattice parameters $a \approx 5.38 \text{ \AA}$, $b \approx 5.39 \text{ \AA}$, and $c \approx 13.2 \text{ \AA}$ in the orthorhombic setting (space group $Bmab$, $I4/mmm$ above structural ordering temperature T_N), depending on doping. At doping values of $x \lesssim 0.06$, incommensurate magnetic order and low-energy fluctuations can be observed at $\mathbf{Q} = (1 \pm \delta, 0, 0)$, $(0, 1 \pm \delta, 0)$. At higher doping values, above the onset of bulk superconductivity, a 45° rotation of the magnetic ordering vector occurs, i.e., $\mathbf{Q} = (1 \pm \delta, \pm \delta, 0)$, $(\pm \delta, 1 \pm \delta, 0)$ [21], see the insets in Figs. 3(d) and 3(f), and the SM for details [24].

III. RESULTS AND DISCUSSION

Although the incommensurability, δ , is very small in the doping regime of this work, we were able to distinguish the

incommensurate peaks in all our samples, see Figs. 3(a)–3(c). All data were fitted with the same double Gaussian model with equal amplitudes and widths for the two peaks. The data were normalized to absolute units using the intensity of the acoustic phonons following the procedure proposed by Xu *et al.* [32]. This allows for a direct quantitative comparison between generalized magnetic susceptibilities of samples of different doping. Note that the signal from the LSCO5 sample is roughly twice as large as in the crystals of higher dopings. In regard to the low-energy magnetic fluctuations, we likewise observe that LSCO5 shows a generalized spin susceptibility that is approximately twice as large as in LSCO6 and LSCO7, see Figs. 3(d)–3(f). No gap opening occurs down to the lowest energy transfers measured, $\hbar\omega = 0.4 \text{ meV}$, in any of the crystals. This behavior is reminiscent of other cuprate materials that display static order, see for example Refs. [8,12,17,33–38]. The absence of a gap, together with the absence of a resonance at higher energies (see Fig. 4 and the discussion below), is compatible with superconductivity in the form of a PDW [12,13].

To further investigate the magnetic behavior in all three crystals, we applied a magnetic field perpendicular to the CuO_2 planes. This causes a clear enhancement of the static signal in LSCO7, see Fig. 3(c), while no discernible effect is seen in the static magnetic signal in LSCO5 and LSCO6, as shown in Figs. 3(a) and 3(b). This leads to the conclusion that the field effect in the elastic channel is largest for the crystal

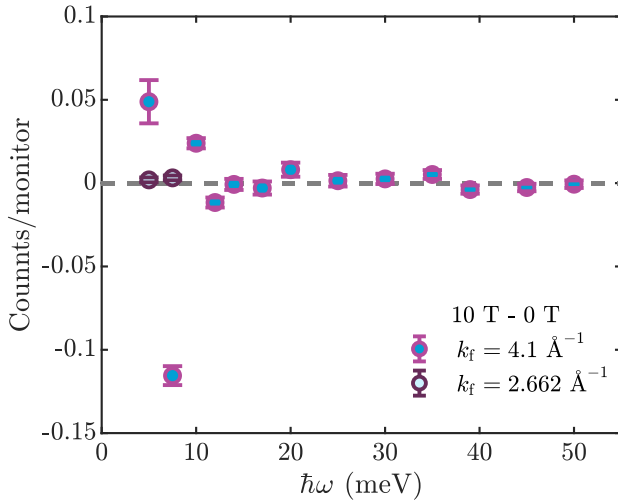


FIG. 4. The effect of a magnetic field on the high-energy fluctuations in LSCO5 measured with neutron scattering at 2 K. Each point is obtained by subtracting the signal at 0 T from the signal at 10 T and integrating over \mathbf{Q} .

that displays the largest superconducting volume fraction. On the other hand, the field effect in the inelastic channel is very similar in all three samples, where we observe a clear decrease of the dynamic susceptibility, $\chi''(\omega)$, for $\hbar\omega < 2$ meV, see Figs. 3(d) and 3(f). This suppression is present at base temperature, whereas the low-energy susceptibility is independent of field at $T = 40$ K.

This leaves us with the remarkable observation that the low-energy response is similar in all samples, albeit different in overall magnitude, regardless of whether a coherent superconducting phase is present or not. This is surprising, given the clear difference of the magnetic field effect on the static signal of the different samples. In LSCO7, the magnetic field suppression of the inelastic signal goes along with an enhancement of the static signal, see Fig. 3(c). Such behavior can generally be interpreted as the slowing-down of spin fluctuations inside vortices of the CuO_2 planes. Intriguingly, our static measurements in LSCO5 or LSCO6 show no such effects. The vortex picture is thus insufficient to explain the data in the case of LSCO5 and LSCO6 and it would be of interest to further investigate what happens to the sub-meV spin fluctuations in this region of the superconducting dome. This will be pursued in future work. For completeness, we have demonstrated that for LSCO5, no spectral weight transfer occurs towards higher energies up to 50 meV, see Fig. 4.

For LSCO7, the temperature dependence of the magnetic field effect on the elastic and inelastic signals is shown in Fig. 5. This reveals that the onset of the field enhancement in the elastic channel occurs at $T_{\text{field}} \geq 25$ K, well above T_c . The field-induced suppression of the fluctuations at $\hbar\omega = 0.8$ meV occurs at the same temperature. This indicates a spectral weight shift from the low-energy magnetic excitations to the elastic channel.

A possible interpretation of the fact that $T_{\text{field}} > T_c$ is that two-dimensional superconducting correlations are present at temperatures above T_c . Indeed, in the $x = 0.07$ doped crystal investigated in Ref. [35], the diamagnetic response for in-

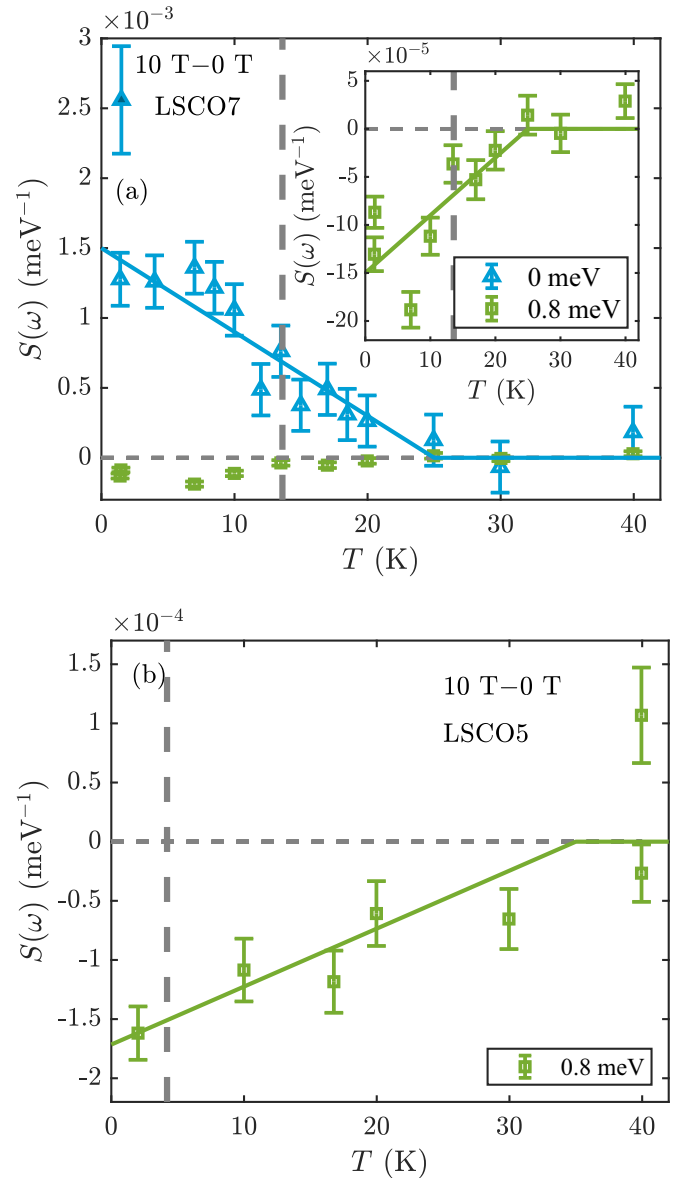


FIG. 5. Temperature dependence of the field effect on magnetic order and fluctuations ($\hbar\omega = 0.8$ meV) in (a) LSCO7 at $Q_{\text{IC}} = (0.93, 0.07, 0)$ and (b) LSCO5 at $Q_{\text{IC}} = (0.95, 0.05, 0)$. The data is shown as point-by-point subtraction of the Brillouin Zone averaged spin correlation function at zero field from that at 10 T. The inset in (a) shows the 0.8 meV data on a smaller scale. The vertical dashed lines denote T_c , and solid lines are guides to the eye.

plane fields occurs prior to the onset of three-dimensional superconductivity. In LSCO5, the onset of the field suppression of the inelastic fluctuations occurs at $T \geq 20$ K, see Fig. 5. This is above the temperature where we observe a drop in the out-of-plane susceptibility indicating that the field effect in LSCO5 is not directly linked to two-dimensional superconducting fluctuations. The general suppression of magnetic fluctuations with field in the underdoped crystals might therefore be due to another, yet unrevealed, common feature in the low-energy correlations. We provide details of the temperature-dependence experiments in the SM [24]. Our findings point toward a gradual emergence of

superconductivity in the underdoped part of the phase diagram both as a function of cooling and as a function of doping. In both cases, two-dimensional superconducting correlations could be the common precursor. Interestingly, a magnetic field applied perpendicular to the CuO_2 planes suppresses the low-energy fluctuations in all three underdoped samples. At the two lowest dopings this is not accompanied by an increase in the static order. These observations are in contrast to what is seen in LSCO of higher dopings where there is solid evidence for strengthening of stripe order and enhancing of low-energy fluctuations upon application of field, see e.g., Refs. [5,7,39,40].

We speculate that the suppression we observe in the low-energy fluctuations is related to the presence of two-dimensional superconducting correlations and a magnetic ordering phenomena which is closely tied to these, as would be the case for a PDW state. However, the details of the mechanism behind the common field-suppression of the low-energy fluctuations remain intriguing. It would be interesting to investigate whether the onset temperature of the fieldsuppression of the fluctuations and field-enhancement of the static signal depends on the strength of the magnetic field. This would be exposed if repeating the measurements presented in Fig. 5 at different magnetic fields between 0 and 10 T.

Lastly, we discuss our findings in relation to other members of the cuprate family. The oxygen-doped cuprate compound $\text{La}_2\text{CuO}_{4+y}$ with a much higher $T_c = 42$ K also displays an ungapped spectrum [41,42] and a weak magnetic field suppression of the low-energy fluctuations [38]. A similar behavior was also found in underdoped $\text{YBa}_2\text{Cu}_3\text{O}_{6.45}$ with $T_c = 35$ K [34]. Common for the above-mentioned systems, as well as for LBCO [43], is that low-energy fluctuations become prominent at low temperatures ($T < T_c$) and suppressed by an applied magnetic field. Notably, this behavior is observed for cuprates at vastly different positions in the phase diagram and could be compatible with a PDW state. However, we also note that a recent study of YBCO found no conclusive evidence of a PDW state [44].

IV. CONCLUSION

We observe a gradual emergence of superconductivity in the underdoped part of the phase diagram of LSCO manifested as an onset of 2D superconducting correlations at the smallest doping, where no bulk SC is observed (LSCO5), and changes in the magnetic spectrum upon application of a magnetic field at elevated temperatures, $T > T_c$, in samples where bulk SC is observed (LSCO7). If 2D correlations are a common precursor, this could point toward the existence of a PDW state, as would be furthermore supported by the absence of a spin gap in all of our underdoped samples. Based on this, we propose that the emergence of superconductivity involves both PDW and gradually larger uniform d -wave superconducting regions which are phase-separated from the stripe-ordered regions. The ratio between the two superconducting phases can be tuned by varying the strontium doping of the samples. We highlight the observation that a similar response to a magnetic field is observed across the cuprate family, and that the gradual emergence of superconductivity involving the development of two-dimensional correlations prior to the homogeneous d -wave phase could likewise be universal across the cuprates.

ACKNOWLEDGMENTS

We are grateful for access to neutron beamtime at the ILL neutron facility. A.E.T. was supported through the ILL Ph.D. program. A.T.R. and H.J. acknowledge support from the Carlsberg Foundation. M.E.K. was supported by the EU MSCA program through Grant No. 838926. We thank Jesper Bendix for providing magnetometry measurement time. The project was supported by the Danish National Committee for Research Infrastructure through DanScatt and the ESS-Lighthouse Q-MAT and the Danish Agency for Higher Education and Science. Y.S. thanks the Chalmers Area of Advances-Materials Science and the Swedish Research Council (VR) with a starting Grant (No. 2017-05078) for funding.

-
- [1] J. M. Tranquada, B. J. Sternlieb, J. D. Axe, Y. Nakamura, and S. Uchida, *Nature (London)* **375**, 561 (1995).
- [2] J. M. Tranquada, *Adv. Phys.* **69**, 437 (2020).
- [3] M. Vojta, *Adv. Phys.* **58**, 699 (2009).
- [4] A. J. Millis, S. Sachdev, and C. M. Varma, *Phys. Rev. B* **37**, 4975 (1988).
- [5] J. Chang, N. B. Christensen, C. Niedermayer, K. Lefmann, H. M. Rønnow, D. F. McMorrow, A. Schneidewind, P. Link, A. Hiess, M. Boehm, R. Mottl, S. Pailhes, N. Momono, M. Oda, M. Ido, and J. Mesot, *Phys. Rev. Lett.* **102**, 177006 (2009).
- [6] B. Lake, G. Aeppli, T. E. Mason, A. Schröder, D. F. McMorrow, K. Lefmann, M. Ishiki, M. Nohara, H. Takagi, and S. M. Hayden, *Nature (London)* **400**, 43 (1999).
- [7] B. Lake, G. Aeppli, K. N. Clausen, D. F. McMorrow, K. Lefmann, N. E. Hussey, N. Mangkorntong, M. Nohara, H. Takagi, T. E. Mason, and A. Schröder, *Science* **291**, 1759 (2001).
- [8] J. Chang, A. P. Schnyder, R. Gilardi, H. M. Rønnow, S. Pailhes, N. B. Christensen, C. Niedermayer, D. F. McMorrow, A. Hiess, A. Stunault, M. Enderle, B. Lake, O. Sobolev, N. Momono, M. Oda, M. Ido, C. Mudry, and J. Mesot, *Phys. Rev. Lett.* **98**, 077004 (2007).
- [9] D. J. van Harlingen, *Rev. Mod. Phys.* **67**, 515 (1995).
- [10] J. M. Tranquada, G. D. Gu, M. Hücker, Q. Jie, H.-J. Kang, R. Klingeler, Q. Li, N. Tristan, J. S. Wen, G. Y. Xu, Z. J. Xu, J. Zhou, and M. v. Zimmermann, *Phys. Rev. B* **78**, 174529 (2008).
- [11] P. M. Lozano, T. Ren, G. D. Gu, A. M. Tsvelik, J. M. Tranquada, and Q. Li, *Phys. Rev. B* **106**, 174510 (2022).
- [12] Z. Xu, C. Stock, S. Chi, A. I. Kolesnikov, G. Xu, G. Gu, and J. M. Tranquada, *Phys. Rev. Lett.* **113**, 177002 (2014).
- [13] M. H. Christensen, H. Jacobsen, T. A. Maier, and B. M. Andersen, *Phys. Rev. Lett.* **116**, 167001 (2016).
- [14] E. Berg, E. Fradkin, S. A. Kivelson, and J. M. Tranquada, *New J. Phys.* **11**, 115004 (2009).
- [15] D. F. Agterberg, J. S. Davis, S. D. Edkins, E. Fradkin, H. D. J. Va, S. A. Kivelson, P. A. Lee, L. Radzihovsky, J. M. Tranquada, and Y. Wang, *Annu. Rev. Condens. Matter Phys.* **11**, 231 (2020).
- [16] B. Lake, H. M. Rønnow, N. B. Christensen, G. Aeppli, K. Lefmann, D. F. McMorrow, P. Vorderwisch, P. Smeibidl,

- N. Mangkorntong, T. Sasagawa, M. Nohara, H. Takagi, and T. E. Mason, *Nature (London)* **415**, 299 (2002).
- [17] M. Kofu, S.-H. Lee, M. Fujita, H.-J. Kang, H. Eisaki, and K. Yamada, *Phys. Rev. Lett.* **102**, 047001 (2009).
- [18] M. H. Hamidian, S. D. Edkins, S. H. Joo, A. Kostin, H. Eisaki, S. Uchida, M. J. Lawler, E.-A. Kim, A. P. Mackenzie, K. Fujita, J. Lee, and J. C. S. Davis, *Nature (London)* **532**, 343 (2016).
- [19] H. Takagi, T. Ido, S. Ishibashi, M. Uota, S. Uchida, and Y. Tokura, *Phys. Rev. B* **40**, 2254 (1989).
- [20] I. Tanaka, K. Yamane, and H. Kojima, *J. Cryst. Growth* **96**, 711 (1989).
- [21] M. Fujita, K. Yamada, H. Hiraka, P. M. Gehring, S. H. Lee, S. Wakimoto, and G. Shirane, *Phys. Rev. B* **65**, 064505 (2002).
- [22] Z. A. Xu, N. P. Ong, Y. Wang, T. Kakeshita, and S. Uchida, *Nature (London)* **406**, 486 (2000).
- [23] S. Ono, S. Komiyama, and Y. Ando, *Phys. Rev. B* **75**, 024515 (2007).
- [24] See Supplemental Material at <http://link.aps.org/supplemental/10.1103/PhysRevB.107.174514> for details on the susceptibility measurements, as well as additional information about the experimental setup and raw neutron scattering data. The Supplemental Material includes Refs. [31,32,37,42,45–48].
- [25] M. Boehm, P. Steffens, J. Kulda, M. Klicpera, S. Roux, P. Courtois, P. Svoboda, J. Saroun, and V. Sechovsky, *Neutron News* **26**, 18 (2015).
- [26] A. E. Tutueanu, M. Boehm, N. B. Christensen, K. Eliassen, L. Folkers, K. Lefmann, A. T. Rømer, Y. Sassa, W. F. Schmidt, and T. B. Tejsner, Incommensurate magnetic order in underdoped LSCO close to the insulator-superconductor boundary. The neutron scattering data recorded on the ThALES spectrometer at the Institut Laue-Langevin (ILL) are available from <https://doi.ill.fr/10.5291/ILL-DATA.5-41-932> (2018).
- [27] A. E. Tutueanu, M. Boehm, K. Eliassen, K. Lefmann, P. Steffens, and T. B. Tejsner, Detailed study of low-energy spin excitations in underdoped LSCO with $x = 0.08$ (superconducting) and $x = 0.05$ (non-superconducting). The neutron scattering data recorded on the ThALES spectrometer at the Institut Laue-Langevin (ILL) are available from <http://doi.ill.fr/10.5291/ILL-DATA.4-02-526> (2018).
- [28] A. E. Tutueanu, M. Boehm, K. Lefmann, V. A. Neacsu, A. T. Rømer, P. Steffens, and T. B. Tejsner, Study of the normal state magnetic fluctuations in LSCO superconductor under applied magnetic field, The neutron scattering data recorded on the ThALES spectrometer at the Institut Laue-Langevin (ILL) are available from <http://doi.ill.fr/10.5291/ILL-DATA.4-02-546> (2019).
- [29] A. E. Tutueanu, M. Boehm, M. E. Kamminga, K. Lefmann, A. T. Rømer, I. Sanlorenzo, P. Steffens, and T. B. Tejsner, Test of temperature induced static stripes rotation in LSCO at the underdoped quantum critical point, The neutron scattering data recorded on the ThALES spectrometer at the Institut Laue-Langevin (ILL) are available from <http://doi.ill.fr/10.5291/ILL-DATA.5-41-998> (2020).
- [30] A. E. Tutueanu, M. Boehm, K. Lefmann, E. Nocerino, A. Piovano, A. T. Rømer, Y. Sassa, P. Steffens, and T. B. Tejsner, Study of high energy magnetic fluctuations in non-superconducting LSCO under applied magnetic field, Institut Laue-Langevin (ILL), <https://dx.doi.org/10.5291/ILL-DATA.4-02-564> (2020).
- [31] A. E. ȚuȚeanu, T. B. Tejsner, M. E. Lăcătușu, H. W. Hansen, K. L. Eliassen, M. Böhm, P. Steffens, C. Niedermayer, and K. Lefmann, *J. Neutron Res.* **22**, 49 (2020).
- [32] G. Xu, Z. Xu, and J. M. Tranquada, *Rev. Sci. Instrum.* **84**, 083906 (2013).
- [33] M. Matsuda, M. Fujita, S. Wakimoto, J. A. Fernandez-Baca, J. M. Tranquada, and K. Yamada, *Phys. Rev. Lett.* **101**, 197001 (2008).
- [34] D. Haug, V. Hinkov, A. Suchaneck, D. S. Inosov, N. B. Christensen, C. Niedermayer, P. Bourges, Y. Sidis, J. T. Park, A. Ivanov, C. T. Lin, J. Mesot, and B. Keimer, *Phys. Rev. Lett.* **103**, 017001 (2009).
- [35] H. Jacobsen, I. A. Zaliznyak, A. T. Savici, B. L. Winn, S. Chang, M. Hücker, G. D. Gu, and J. M. Tranquada, *Phys. Rev. B* **92**, 174525 (2015).
- [36] A. T. Rømer, J. Chang, N. B. Christensen, B. M. Andersen, K. Lefmann, L. Mähler, J. Gavilano, R. Gilardi, C. Niedermayer, H. M. Rønnow, A. Schneidewind, P. Link, M. Oda, M. Ido, N. Momono, and J. Mesot, *Phys. Rev. B* **87**, 144513 (2013).
- [37] H. Jacobsen, S. L. Holm, M.-E. Lăcătușu, A. T. Rømer, M. Bertelsen, M. Boehm, R. Toft-Petersen, J.-C. Grivel, S. B. Emery, L. Udby, B. O. Wells, and K. Lefmann, *Phys. Rev. Lett.* **120**, 037003 (2018).
- [38] A.-E. ȚuȚeanu, H. Jacobsen, P. Jensen Ray, S. Holm-Dahlin, M.-E. Lăcătușu, T. B. Tejsner, J.-C. Grivel, W. Schmidt, R. Toft-Petersen, P. Steffens, M. Boehm, B. Wells, L. Udby, K. Lefmann, and A. T. Rømer, *Phys. Rev. B* **103**, 045138 (2021).
- [39] M. Frachet, I. Vinograd, R. Zhou, S. Benhabib, S. Wu, H. Mayaffre, S. Krämer, S. K. Ramakrishna, A. P. Reyes, J. Debray, T. Kurosawa, N. Momono, M. Oda, S. Komiyama, S. Ono, M. Horio, J. Chang, C. Proust, D. LeBoeuf, and M.-H. Julien, *Nat. Phys.* **16**, 1064 (2020).
- [40] I. Vinograd, R. Zhou, H. Mayaffre, S. Krämer, S. K. Ramakrishna, A. P. Reyes, T. Kurosawa, N. Momono, M. Oda, S. Komiyama, S. Ono, M. Horio, J. Chang, and M.-H. Julien, *Phys. Rev. B* **106**, 054522 (2022).
- [41] B. O. Wells, Y. S. Lee, M. A. Kastner, R. J. Christianson, R. J. Birgeneau, K. Yamada, Y. Endoh, and G. Shirane, *Science* **277**, 1067 (1997).
- [42] Y. S. Lee, R. J. Birgeneau, M. A. Kastner, Y. Endoh, S. Wakimoto, K. Yamada, R. W. Erwin, S.-H. Lee, and G. Shirane, *Phys. Rev. B* **60**, 3643 (1999).
- [43] J. Wen, Z. Xu, G. Xu, J. M. Tranquada, G. Gu, S. Chang, and H. J. Kang, *Phys. Rev. B* **78**, 212506 (2008).
- [44] I. Vinograd, R. Zhou, M. Hirata, T. Wu, H. Mayaffre, S. Krämer, R. Liang, W. N. Hardy, D. A. Bonn, and M.-H. Julien, *Nat. Commun.* **12**, 3274 (2021).
- [45] S. Wakimoto, S. Lee, P. M. Gehring, R. J. Birgeneau, and G. Shirane, *J. Phys. Soc. Jpn.* **73**, 3413 (2004).
- [46] D. Vaknin, S. K. Sinha, D. E. Moncton, D. C. Johnston, J. M. Newsam, C. R. Safinya, and H. E. King, Jr., *Phys. Rev. Lett.* **58**, 2802 (1987).
- [47] M. Fujita, H. Hiraka, M. Matsuda, M. Matsuura, J. M. Tranquada, S. Wakimoto, G. Xu, and K. Yamada, *J. Phys. Soc. Jpn.* **81**, 011007 (2011).
- [48] A. Hiess, M. Jiménez-Ruiz, P. Courtois, R. Currat, J. Kulda, and F. J. Bermejo, *Physica B* **385-386**, 1077 (2006).